[CANCER RESEARCH 64, 4790–4799, July 15, 2004]

The Tumor Microenvironment Controls Primary Effusion Lymphoma Growth *in Vivo*

Michelle R. Staudt,[1] Yogita Kanan,[2] Joseph H. Jeong,[3] James F. Papin,[1] Rebecca Hines-Boykin,[2] and Dirk P. Dittmer[4]

[1]Graduate Program in Microbiology and Immunology and [2]Department of Microbiology and Immunology, The University of Oklahoma Health Sciences Center, Oklahoma City, Oklahoma; [3]Dana-Farber Cancer Center, Harvard Medical School, Boston, Massachusetts; and [4]Department of Microbiology and Immunology, The University of North Carolina at Chapel Hill, Chapel Hill, North Carolina

ABSTRACT

Certain lymphomas in AIDS patients, such as primary effusion lymphoma (PEL), are closely associated with the lymphotropic γ herpes virus Kaposi's sarcoma-associated herpes virus (KSHV), also called human herpesvirus 8. The virus is thought to be essential for tumorigenesis, yet systems to investigate PEL *in vivo* are rare. Here we describe PEL tumorigenesis in a new xenograft model. Embedded in Matrigel, PEL cells formed rapid, well-organized, and angiogenic tumors after s.c. implantation of C.B.17 SCID mice. Without Matrigel we did not observe comparable tumors, which implies that extracellular support and/or signaling aids PEL. All of the tumors maintained the KSHV genome, and the KSHV latent protein LANA/orf73 was uniformly expressed. However, the expression profile for key lytic mRNAs, as well as LANA-2/vIRF3, differed between tissue culture and sites of implantation. We did not observe a net effect of ganciclovir on PEL growth in culture or as xenograft. These findings underscore the importance of the microenvironment for PEL tumorigenesis and simplify the preclinical evaluation of potential anticancer agents.

INTRODUCTION

Kaposi's sarcoma-associated herpesvirus (KSHV), also called human herpesvirus 8 (HHV-8), is a B-cell-tropic human herpesvirus (reviewed in Refs. 1, 2). The virus was first discovered in 1994 in Kaposi's sarcoma (KS) tumors of AIDS patients. In AIDS patients, KSHV is also associated with two lymphoproliferative disorders, namely, primary effusion lymphoma [PEL; initially called body cavity based lymphoma (BCBL); Ref. 3] and multicentric Castleman's disease (4). To date, multiple KSHV isolates have been sequenced and been shown to contain a 120-kb central long unique region encoding ~80 putative open reading frames (5–7). Antibodies against KSHV exist in virtually all of the HIV-infected as well as in HIV-uninfected KS patients. Prospective longitudinal studies found that increases in peripheral-blood viral load as well as KSHV-specific antibody titers precede the onset of disease and correlate with increased risk for KS. These observations argue that KSHV is required for disease manifestation, although a particular molecular mechanism, the exact requirement for KSHV in tumor development (tumor initiation *versus* tumor progression), or specific viral oncogenes have not been unequivocally established.

In endothelial-lineage KS lesions, KSHV is present in every tumor cell at 10–20 copies of the viral episome per cell (8–11). Most KS tumor cells are latently infected, but low percentages of KSHV-infected cells undergo random lytic reactivation, lytic protein expression, and lytic DNA replication (10, 12). Depending on the stage of the lesion (plaque, patch, or nodal) KS can be monoclonal or oligoclonal in origin (13–15), and conflicting studies have been published. This underscores the difficulty in studying the role of KSHV in KS. Despite a multiyear effort, less than a handful KS-derived cell lines have been adapted to continued growth in culture, because KS biopsy explants tend to lose the virus upon passage in culture (16, 17). Unlike primary tumors, KS-derived culture-adapted cells are aneuploid, have accumulated multiple translocations, and have lost the KSHV episome during the culture process (18–21). Presumably, this outcome reflects different selection pressures in different environments: growth on a plastic substrate selects for fully transformed tumor cells that acquire additional mutations and, therefore, no longer depend on viral oncogenes and no longer need to maintain the viral episome. These KS tumor-derived, KSHV-negative cell clones cannot be used to study the contribution of KSHV to KS. Experimental infection of primary or life-extended endothelial cell culture mimics the opposite sequence of events, because the cells are cell culture-adapted before infection. A number of endothelial cell culture models maintain KSHV after experimental infection for some time (22–25), and infection of cell culture endothelial cells represents one approach to studying KS oncogenesis. Flore *et al.* (26) examined the infection of cultured primary vascular endothelial by KSHV and reported that over time these cells gave rise to transformed clones. KSHV-infected endothelial cell populations ordinarily do not form tumors in nude mice, unless other oncogenes, such as human papilloma virus E6/E7 or telomerase, are also present (22, 23). These observations led to the development of the paracrine hypothesis for KS pathogenesis in which KSHV induces a growth-factor rich microenvironment that supports continued proliferation of KSHV latently infected as well as neighboring, uninfected tumor cells (21, 27–31).

In contrast to KSHV-associated endothelial lineage tumors, stable 100% KSHV-positive suspension cell lines are readily established from KSHV-associated B cell-lineage tumors such as PEL (3, 32–39). All of the PEL are monoclonal and usually arise in patients with advanced HIV disease, often in conjunction with KS. Although PEL came to prominence as an AIDS-associated malignancy, incidences of PEL have also been reported in HIV-negative men and women (40). With the advent of highly active antiretroviral therapy, the incidence of AIDS-associated cancers has decreased in the United States, but PEL cases are regularly encountered in countries of high KSHV prevalence, such as Italy, or in individuals who do not have access to anti-HIV treatment or prevention programs. It is possible that as highly active antiretroviral therapy failures mount, we will again see an increased incidence of PEL in $KSHV^+/HIV^+$ patients. Hence, there is a continued need for the development of therapeutics against KSHV-associated lymphomas. PEL cell lines represent the most consistent model in which to study KSHV biology. These cell lines grow indefinitely in culture with or without human interleukin 6 as a supplement. Importantly, every single lymphoma cell maintains the KSHV episome and expresses the viral latency associated nuclear

Received 12/8/03; revised 4/8/04; accepted 5/19/04.

Grant support: Roche Organ Transplant Foundation (ROTRF129387254), the National Cancer Institute (CA109232), and contracts from the AIDS Malignancy Consortium (CA700580 and CA-03–017) to D. Dittmer. J. Papin was supported by NIH Training Grant T32 AI07364 and M. Staudt by NIH Training Grant T32 AI007633 to the Department of Microbiology and Immunology at University of Oklahoma Health Sciences Center.

The costs of publication of this article were defrayed in part by the payment of page charges. This article must therefore be hereby marked *advertisement* in accordance with 18 U.S.C. Section 1734 solely to indicate this fact.

Requests for reprints: Dirk P. Dittmer, The University of North Carolina at Chapel Hill, CB# 7290, 804 Mary Ellen Jones, Chapel Hill, NC 27599-7290. Phone: (919) 966-1191; Fax: (919) 962-8103; E-mail: dirkdittmer@mac.com.

antigen LANA/orf73 (41–49). In these PEL cell lines, the viral load is around 50–100 latent episomes per cell (50), which is significantly higher than in KS lesions. About half of the available PEL cell lines are coinfected with EBV as well as with KSHV (39, 40, 51–54). Stable PEL cell lines have been derived from HIV-positive as well as HIV-negative patients, which suggests that HIV did not contribute to B-cell tumorigenesis in the latter instances. Although KSHV is predominantly latent in the PEL cell lines, it can be induced to undergo lytic replication by treatment with phorbolester, calcium ionophores, sodium-butyrate, IFN-γ or coinfection with human cytomegalovirus (37, 52, 55–63).

The use of tissue culture as a single model for KSHV-associated cancers is limited in that significant events in KSHV pathogenesis may be underappreciated, because they do not take place in cell culture. Therefore, many investigators have tried to establish animal models for the study of PEL and KSHV. Because KSHV replicates exclusively in human cells, there are only two established rodent models with which to study KSHV-dependent lymphomagenesis: either normal human tissue is engrafted onto severe combined immunodeficiency (SCID) mice followed by injection of purified KSHV virions (35, 64, 65), or KSHV-infected human tumor cells, such as PEL, are injected into immunodeficient SCID or nude mice (34, 59, 66). We showed previously that inoculation of chimeric SCID-hu Thy/Liv mice with purified KSHV virions resulted in lytic replication followed by long-term latency. In this model, lytic and latent KSHV transcription was restricted to $CD19^+$ human B-cells (64) reflecting the lymphotropism of the virus. Systemic administration of ganciclovir to KSHV-infected SCID-hu mice inhibited lytic viral replication in the implant. However, mice infected with cell-free virus did not develop tumors. Alternatively, several groups have reported on the behavior of KSHV-positive PEL tumor cells in mouse xenograft systems. i.p. injection of the KS-1 PEL cell line ($KSHV^+$ EBV^-) led to ascites tumors (67). Different PEL injection sites were studied by Boshoff *et al.* (39) who showed that injection of the PEL cell lines HBL-6 ($KSHV^+$ EBV^+) and BCP-1 ($KSHV^+$ EBV^-) i.v., i.p., or s.c., likewise led to tumor formation in the mice. Picchio *et al.* (35) found that i.p. or s.c. injection of the PEL cell line BCBL-1 ($KSHV^+$ EBV^-) led to ascites as well as s.c. tumors, whereas implantation of KSHV-exposed normal human PBMCs did not elicit a phenotype, confirming that in contrast to EBV, KSHV cannot transform peripheral B lymphocytes (63, 68). Common to all three of the studies, PEL-derived tumors grew extremely poorly with a mean tumor latency period of $\geq$50 days per 10^6 cells in a challenge dose. This is in contrast to rapid progression of PEL growth in patients or EBV^+ Burkitt's lymphoma cell line growth in xenograft models (69, 70). Such a phenotype suggests that in the case of PEL, like in the case of KS, the microenvironment surrounding the KSHV-infected cell may play a critical role in tumor progression.

In trying to study the influence of the host environment on tumor growth, we initially observed that tumor growth accelerated if $KSHV^+$ PEL cells (BCBL-1) were injected topically near the abdominal wall or beneath the kidney capsule compared with s.c. or i.p. injection.[5] These observations argued in favor of the aforementioned model that KSHV-infected PEL cells respond to environmental factors, which may be soluble (cytokines) or mechanical (extracellular matrix) in nature. To explore this conjecture, the studies presented herein test the hypothesis that growth factor-depleted extracellular matrix (Matrigel) enhances ectopic tumor formation by $KSHV^+$/EBV^- BCBL-1 cells. We observed much more rapid growth of PEL cells s.c. in SCID mice in the presence of Matrigel compared with injection of PEL cells without Matrigel. This outcome shows that PEL tumor growth *in vivo* is dependent on the presence of extracellular matrix. Furthermore, these studies establish a tractable small animal model to study KSHV lymphomagenesis. In this model, ganciclovir did not inhibit PEL tumor formation. The novel animal model described in this report should facilitate *in vivo* screening and validation of other anti-KSHV and anticancer drugs.

MATERIALS AND METHODS

Cell Culture. The BCBL-1 cell line was obtained from Don Ganem (University of California San Francisco, San Francisco, CA). The cells were routinely cultured in RPMI 1640 supplemented with 100 μg/ml streptomycin sulfate, 0.25 μg/ml amphotericin B, 100 units/ml penicillin G (Invitrogen Life Technologies, Inc., Carlsbad, CA), 2 mM L-glutamine, 0.05 mM 2-mercaptoethanol, and 0.075% sodium bicarbonate at 37°C in 5% CO_2. To test the *in vitro* effects of Ganciclovir on BCBL-1 cells, 3×10^6 cells were resuspended in the presence of 390 μM (CC_{50} equivalent), 39 μM (IC_{90} equivalent), and 3.9 μM Ganciclovir (IC_{50} equivalent; Sigma Inc., St. Louis, MO), and 20 ng/ml TPA (Calbiochem Inc., San Diego, CA) as described previously (52, 71). The cell numbers and viability were determined by trypan blue stain.

Tumor Formation. Cells were counted, washed once in ice-cold PBS (Cellgro Mediatech, Inc., Herndon, VA), and indicated cell doses were diluted in 200 μl PBS or 200 μl growth factor-depleted Matrigel (BD Biosciences, Bedford, MA). Cells were injected s.c. into the right flank or i.p. into C.B.-17 SCID mice (The Jackson Laboratory, Bar Harbor, ME). The mice were observed every 2 days for the presence of palpable tumors. In experiments studying the effect of Ganciclovir, mice were injected with 5×10^6 BCBL cells containing 200 μl Matrigel s.c. and were also injected i.p. with 2 mg/10g/day Ganciclovir (Sigma-Aldrich Corp., St. Louis, MO) and observed for the tumor formation. This dosing follows our protocol established previously (64). Ganciclovir was dissolved at 1 mg/ml in PBS and adjusted to pH 8.0 with 1 N NaOH at 65°C, filtered-sterilized through a 0.2-μm filter (Acrodisk), and stored at 4°C for the duration of the experiment. The tumors were excised from the site of injection and were either fixed in formalin (Fisher Diagnostics, Middletown, VA) or resuspended in TRI reagent (Sigma-Aldrich Corp.) and processed for reverse transcription-PCR.

RNA Isolation and Reverse Transcription. Total RNA from suspension cells was isolated by using the Absolutely RNA Microprep kit (Stratagene, La Jolla, CA). Solid tumor pieces were resuspended in 750 μl TRI Reagent (Sigma-Aldrich Corp.) and disrupted using a Ultra-Turrax T8 (IKA Labortechnik, Staufen, Germany). RNA was isolated according to the supplier's protocol, precipitated, and resuspended in 50 μl diethyl pyrocarbonate-treated water at 56°C for 10 min. Subsequently, DNA was removed from the RNA isolation by using the DNA-free RNA kit (Zymo Research, Orange, CA). The RNA was reverse transcribed as described (43) in a 20-μl reaction with 100 units of Moloney murine leukemia virus reverse transcriptase (Life Technologies, Inc.), 2 mM deoxynucleoside triphosphates, 2.5 mM $MgCl_2$, 1 unit RNAsin (all from Applied Biosystems, Foster City, CA), and 0.5 μg of random hexanucleotide primers (Amersham Pharmacia Biotech, Piscataway, NJ). The reverse transcription reaction was sequentially incubated at 42°C for 45 min, 52°C for 30 min, and 70°C for 10 min. The reaction was stopped by heating at 95°C for 5 min. Finally, 0.5 μl of RNase H (Life Technologies, Inc.) was added to the reverse transcription reaction, which was then incubated at 37°C for 30 min, heat-inactivated at 70°C for 10 min, and cDNA pools stored at −80°C.

Real-Time Quantitative PCR. Quantitative real-time PCR primers were designed using Primer Express 1.5 (Applied Biosystems) and used as described previously (43, 72) on an ABI PRIZM 7700 Sequence Detector (Applied Biosystems) using universal cycling conditions (2 min at 50°C, 10 min at 95°C, followed by 40 cycles of 15 s at 95°C and 1 min at 60°C). The cycle-threshold values were determined by automated analysis. The threshold was set to five times the SD of the nontemplate control. Dissociation curves were recorded after each run, and the amplified products were routinely analyzed by 2% agarose gel electrophoresis (73).

Immunohistochemistry. Seven μm paraffin sections of fixed tumor tissue were stained with H&E stains. H&E (Vector Laboratories, Burlingame, CA) staining was done by de-paraffinization of the sections using histoclear (Sigma-Aldrich Corp.) followed by staining with hematoxylin for 15 min then a

[5] P. Dittmer, C. Stoddard, and D. Ganem, unpublished observations.

20-min water wash. The slides were subsequently stained with eosin for 2 min, dehydrated in 95% alcohol and absolute alcohol, cleared in xylene, and mounted in Permount (Sigma Inc.). LANA was detected using a monoclonal rat anti-LANA antibody (Ref. 47; 1:10 dilution, from Applied Bioscience Inc.) and goat antirat horseradish peroxidase (Kirkegaard & Perry, Inc. Gaithersburg, MD) and visualized using horseradish peroxidase Substrate-Chromogen mixture (Zymed Laboratories, San Francisco, CA). Proliferating cell nuclear antigen was detected using rabbit antiproliferating cell nuclear antigen antibody (FL261; Santa Cruz Biotechnology Inc., Santa Cruz, CA) and cyclin-D using rabbit anti-cyclin-D1 antibody (M-20; Santa Cruz Biotechnology Inc.) and goat antirabbit horseradish peroxidase (Kirkegaard & Perry, Inc.). Slides were counterstained with hematoxylin, dehydrated in 95% alcohol and absolute alcohol, cleared in xylene, and mounted in Permount (Sigma Inc.).

Statistical Analysis. Calculations were performed using Excel (Microsoft Inc., Redwood, WA) and SPSS v11.0 (SPSS Science, Chicago, IL). Hierarchical clustering was performed as described previously (72). All of the samples were normalized to gapdh, centered by median of gene, normalized to ± 1, and ordered by hierarchical clustering using ArrayMiner software (Optimal Design Inc., Brussels, Belgium).

RESULTS

Matrigel Enables Rapid, s.c. Growth of PEL in SCID Mice. In human patients, PEL are found in the pleural or abdominal cavities. Previous studies have reported the successful propagation of PEL cells as ascites tumors in mice (35, 39). In contrast to EBV^+ lymphomas or EBV^+ lymphoblastoid cell lines (reviewed in Ref. 70), $KSHV^+$ PEL grew extremely slowly with a mean time-to-tumor-formation of ~2 months despite injection of a large dose ($>10^6$) of cells per animal. The progression of i.p. tumors is difficult to measure by noninvasive methods, and as such their use for quantitative studies is limited. To circumvent these limitations, we attempted to establish a s.c. tumor model of $KSHV^+$ PEL in SCID mice. However, when SCID mice were injected s.c. with 5×10^5, 5×10^6, or 5×10^7 BCBL-1 cells, none of the mice developed tumors (Table 1, Experiment #1). This outcome was consistent with earlier observations that reported a mean time-to-tumor-formation of PEL cells injected into mice s.c. of ~2 months (35, 39). Because PELs naturally reside in the pleural cavity of human patients and not in a s.c. environment, we reasoned that a suitable microenvironment would augment PEL growth. To test this hypothesis, we repeated the PEL injections into SCID mice with the addition of Matrigel to the inoculum. Matrigel is a growth factor-depleted extracellular matrix material that can enhance the growth of substrate-dependent cells *in vitro* and *in vivo*. By itself, Matrigel did not induce tumors in mice (Table 1, Experiment #1), but after 1 week, 1 mouse that had received 5×10^6 BCBL-1 cells in Matrigel via s.c. injection developed a tumor (Table 1, Experiment #2). Albeit not statistically significant ($P \geq 0.2$, by t test), this outcome indicated that Matrigel may enable the s.c. growth of PEL.

To additionally characterize the effect of Matrigel on BCBL-1 growth, we repeated the experiment at a dose of 5×10^6 BCBL-1 cells in Matrigel and extended the observation period (Table 1, Experiments #3 and #4). Tumors were observed in 6 of the 7 mice treated with both BCBL-1 cells and Matrigel. In contrast, none of the mice that received BCBL-1 cells without Matrigel developed tumors even after 28 days. This demonstrates that Matrigel enhances tumor formation by BCBL-1 cells ($P \leq 0.0005$, by t test) in the s.c. microenvironment of SCID mice. The combination of PEL and Matrigel presents the fastest *in vivo* model to study $KSHV^+$ PEL tumorigenesis to date.

In the same series of experiments with more animals, 13 SCID mice were injected i.p with 5×10^6 BCBL-1. Nine of the mice developed tumors within 28 days (Table 1, Experiment #3), which is significantly different from the zero mice with tumors derived from s.c. injected BCBL-1 cells ($P \leq 0.0001$, by t test), and implies that the BCBL-1 cell line maintained its dependence on pleural cavities or some other supportive environment *in vivo*. The observation that BCBL-1-derived tumors develop more rapidly in the presence of Matrigel in the s.c. microenvironment of the mouse compared with without Matrigel suggests that Matrigel may be a capable substitute for the pleural environment. To account for different mouse cohorts and variations in the BCBL-1 preparation, we repeated the experiment a third time. Five mice were injected s.c. with 5×10^6 BCBL-1 in 0.2 ml of Matrigel, and 5 mice were injected s.c. with 5×10^6 BCBL cells in PBS without Matrigel (Table 1, Experiment #4). As observed in the previous experiments, all of the mice that received BCBL-1 cells with Matrigel developed tumors by day 14. Among the mice injected s.c. with BCBL-1 cells without Matrigel, 1 animal developed a tumor after 19 days. A second mouse developed a tumor on day 24, and the remaining mice did not develop lesions at all ($P \leq 0.0005$, by t test).

To quantify the growth differential of Matrigel on BCBL-1 s.c. tumor formation, we performed Kaplan-Meier analysis. Fig. 1*A* compares C.B.-17 SCID mice that were injected s.c. with BCBL-1 cells alone to animals that were injected with BCBL-1 cells plus Matrigel. None of the mice injected s.c. with BCBL-1 cells developed tumors by 1 month. In contrast, 2 of the 7 mice that received BCBL-1 cells in Matrigel developed tumors by day 6 (71% tumor free), 4 of 7 mice had developed tumors by day 10 (43% tumor free), 6 of 7 mice by day 12 (14% tumor free), and all of the mice had developed tumors by day

Table 1 *Tumor formation of BCBL-1 cells in SCID mice*

Significance was determined by independent samples *t* test.

Exp.	Dose	Route	Treatment	Animals	Time	No. of tumors	% tumors	Significance ($P \leq$)
1	5.0E +05	s.c.	-	4	7	0	0%	
	5.0E +06	s.c.	-	3	7	0	0%	
	5.0E +07	s.c.	-	4	7	0	0%	
	None	s.c.	Matrigel	2	7	0	0%	
2	5.0E +05	s.c.	Matrigel	4	7	0	0%	-
	5.0E +06	s.c.	Matrigel	3	7	1	33%	0.2113
	5.0E +07	s.c.	Matrigel	4	7	0	0%	
3	5.0E +06	s.c.	-	5	28	0	0%	-
	5.0E +06	s.c.	Matrigel	7	14	6	86%	0.0005
	5.0E +06	i.p.	-	13	28	9	69%	0.0001
4	5.0E +06	s.c.	-	5	14	0	0%	-
	5.0E +06	s.c.	Matrigel	5	14	5	100%	0.0005
5	5.0E +06	s.c.	Matrigel	5	14	5	100%	-
	5.0E +06	s.c.	Matrigel and ganciclovir	5	14	5	100%	1.0000
6	5.0E +06	s.c.	Matrigel	4	14	4	100%	-
	5.0E +06	s.c.	Matrigel and ganciclovir	4	14	4	100%	1.0000

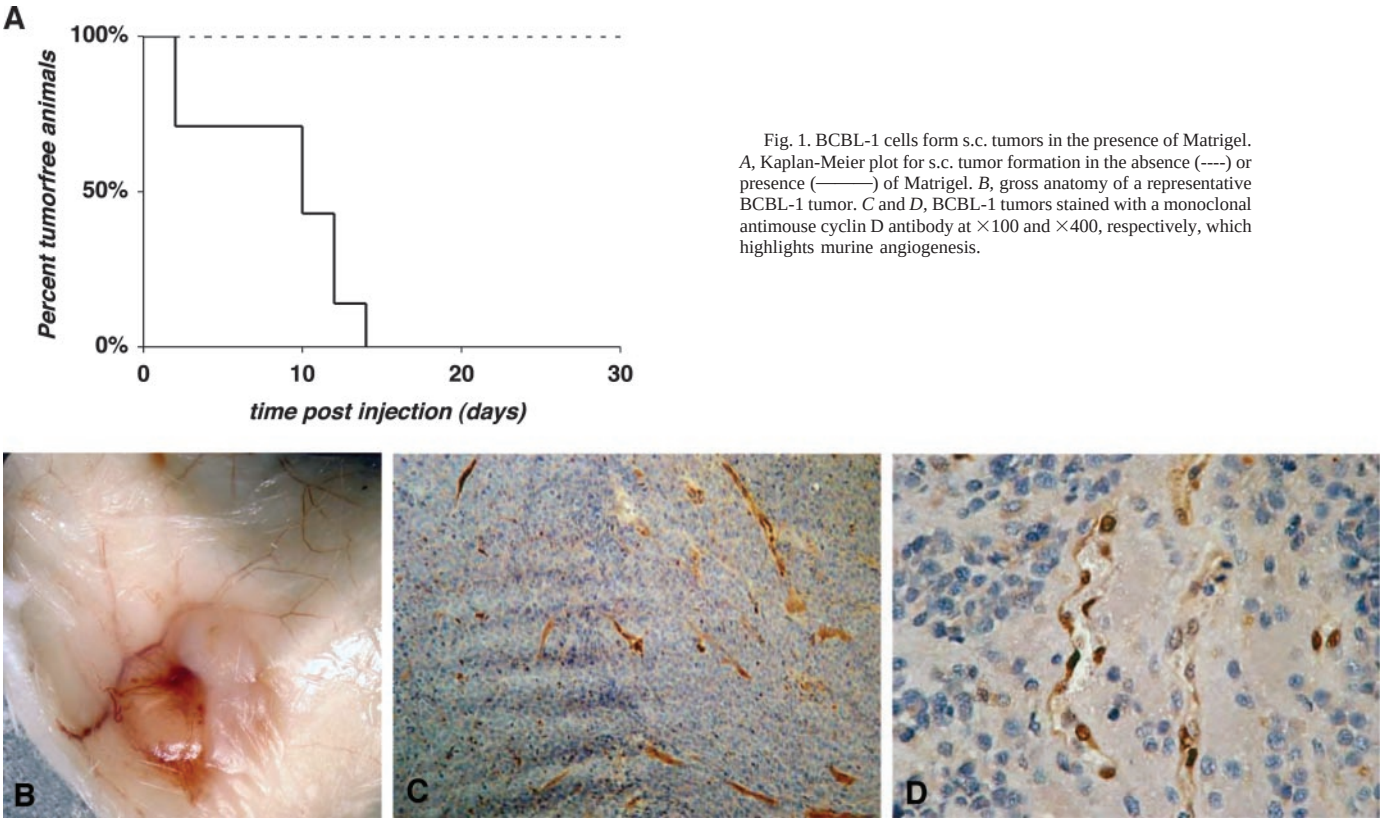

Fig. 1. BCBL-1 cells form s.c. tumors in the presence of Matrigel. *A*, Kaplan-Meier plot for s.c. tumor formation in the absence (----) or presence (———) of Matrigel. *B*, gross anatomy of a representative BCBL-1 tumor. *C* and *D*, BCBL-1 tumors stained with a monoclonal antimouse cyclin D antibody at ×100 and ×400, respectively, which highlights murine angiogenesis.

14 (0% tumor free; $P \leq 0.0005$, by log-rank test). These data demonstrate that: (*a*) PEL are dependent on extracellular support for *in vivo* tumor formation; (*b*) growth factor-depleted Matrigel can provide such support as efficiently as the pleural cavity; and (*c*) PEL can be propagated s.c., which facilitates the ease of tumor observations.

Upon gross examination, BCBl-1 tumors could induce murine angiogenesis as evident by the red blood vessels leading to the tumor implant (Fig. 1*B*). The blood vessels and capillary endothelial cells were of murine origin as determined by immunohistochemical staining of BCBL-1 tumors with a rat monoclonal antibody specific for mouse cyclin D (Fig. 1, *C* and *D*). This phenotype was expected based on the long history of human xenograft tumors in SCID mice (70) and emphasizes that the principal angiogenic signals are conserved across species.

Because some rare tumors did eventually form after s.c. injection of BCBL-1 cells without Matrigel, we asked if these tumors were phenotypically different compared with BCBL-1 tumors formed after s.c. injection of BCBL-1 plus extracellular support via Matrigel. While comparing BCBL-1 cells growing in these three environments (i.p., s.c., or s.c. plus Matrigel), striking morphological differences became evident. BCBL-1 i.p. tumors were observed to be irregular by H&E staining, with empty spaces and necrosis evident (Fig. 2, *C* and *D*). In addition, individual nucleoli were prominent, perhaps suggesting blastic differentiation. In contrast, Matrigel-supported tumors exhibited a regular appearance with many uniformly stained small cells and inconspicuous nuclei (Fig. 2, *E* and *F*). As seen in Fig. 1, these tumors were well vascularized. Under low magnification the organizing effect of the Matrigel becomes more evident and can be used to discern between s.c. tumors with or without Matrigel. The very few tumors that formed after s.c. injection in the absence of Matrigel also showed extensive necrosis but dense nuclei (Fig. 2, *A* and *B*). This observation confirms that Matrigel forms a lattice in which the tumor cells can grow in an orderly fashion, which could provide a more even flow of oxygen and nutrients and could help explain the accelerated rate of tumor formation in mice injected with both BCBL-1 cells and Matrigel.

Because LANA is expressed in every PEL cell in suspension culture, we wanted to determine whether LANA was also expressed in PEL-derived tumors in mice. The few aberrant tumors that developed in the absence of Matrigel maintained LANA expression, but LANA-negative foci were also observed (Fig. 3*A*). In contrast, tumors that formed after i.p. injection of BCBL-1 cells expressed LANA protein uniformly in all of the cells (Fig. 3*B*). LANA expression likewise was uniform in Matrigel-supported s.c. tumors (Fig. 3*C*). Taken together, the histochemical analysis revealed that the peritoneal cavity imposes a different environment on BCBL-1 cells as s.c. implantation even with Matrigel. Specifically, i.p. growth induces immunoblastic activation of PEL and KSHV viral reactivation (see below). Ectopic *in vivo* growth, such as experienced upon s.c. injection without Matrigel, selected for fast-growing clones, which no longer resembled the inoculums, and many lost LANA expression (analogous to KS biopsy explant cultures; Ref. 16). In contrast, Matrigel enabled uniform growth of LANA-positive PEL cells after s.c. injection but without overt differentiation.

KSHV Transcription in PEL Implants. To asses the fate of KSHV in the three different microenvironments (i.p., s.c., or s.c. plus Matrigel), we performed real-time quantitative reverse transcription-PCR using a set of primers described previously (43). These primers query representative members of the various KSHV kinetic transcriptional classes (α, β, and γ), which we and others defined previously for KSHV in PEL (41–43, 74) and which most consistently predict the stage of the KSHV life cycle for all of the known PEL isolates. The assay is highly specific, because in addition to the outside primers, hybridization to a third sequence-specific probe (TaqMan) is required to obtain a signal. To limit variation, we used multiplexing and coamplified either gapdh or LANA as an internal control in the same

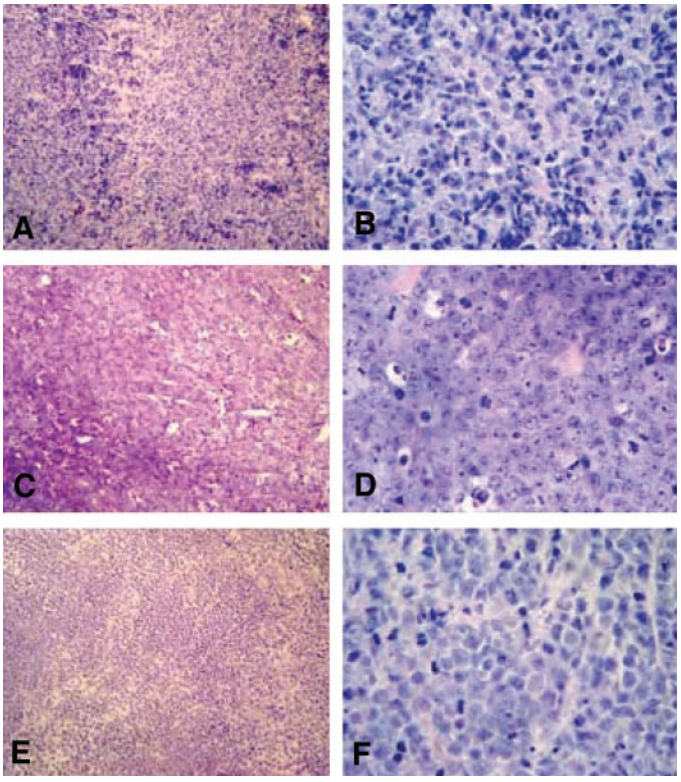

Fig. 2. H&E stain of BCBL-1 tumors. *A* and *B*, ×40 and ×400 magnification of a representative s.c. tumor. *C* and *D*, ×40 and ×400 magnification of a representative i.p. tumor. *E* and *F*, ×40 and ×400 magnification of a representative Matrigel-enhanced s.c. tumor.

reaction tube, the signal of which was quantified using a different fluorophor. Our molecular profiling uncovered significant differences for the three tumor types (Fig. 4). First, the mRNA for the latent gene *LANA* was abundantly transcribed in all three of the tumor types at ~50% the level of gapdh mRNA, which corroborates our observations of BCBL-1 cells in culture (43, 75). Second, primers directed against the v-cyclin open reading frame (vCyc/orf72) likewise detected equivalent mRNA levels in each tumor class. This is expected, because LANA and vCyc mRNAs are coregulated and 3′-coterminal (12, 75). In contrast to both LANA and v-cyclin, LANA-2/vIRF3 is a latent mRNA that is only present in the KSHV-infected B-cells (MCD and PEL) but not in KSHV-infected endothelial cells such as KS (49, 72). LANA-2 mRNA levels were significantly ($P \leq 0.07$, by t test) higher in the i.p. tumor cohort compared with s.c. and s.c. plus Matrigel tumors, although in culture all of the BCBL-1 cells transcribe LANA-2/vIRF-3. Also, the mRNA levels for Rta/orf50 and vGPCR/orf74 were significantly higher in i.p. tumors compared with s.c. and s.c. plus Metrogel tumors. This observation is consistent with the more immunoblastic phenotype of the i.p. tumor class. The mRNAs level for orf57, another lytic gene showed a similar trend, but the differences did not reach significance levels below $P \leq 0.07$. These results argue that, whereas all of the tumors transcribed the canonical viral latent genes, BCBL-1 cells grown as i.p. tumors became activated and transcribed several early lytic mRNAs, whereas BCBL-1 cells grown as s.c. tumors did not. The s.c. plus Matrigel tumors also showed elevated levels of lytic gene expression, which was similar to i.p. tumors. The LANA-2/vIRF-3 mRNA was only present in the environment of the peritoneal cavity. This suggests that the Matrigel s.c. environment and the peritoneal cavity exude different signals that can induce a corresponding adaptation in KSHV gene expression. The few aberrant tumors that developed ectopically in the s.c. microenvironment in the absence of extracellular support (Matrigel) or cytokines only expressed latent viral genes.

Ganciclovir Slows PEL Tumor Formation in Mice. Nucleoside analogs, such as ganciclovir, inhibit the KSHV polymerase (orf9; Refs. 55, 64, 71, 76, 77). A clinical study suggested that ganciclovir has a beneficial effect on KSHV-associated malignancies, because it seems to lower tumor burden and spread in KS patients (78). However, its mechanism of action with regard to antitumor activity is unknown. Ganciclovir can act by several different means to inhibit KSHV pathogenesis. The drug could act to limit peripheral viremia, which would inhibit the latent establishment of KSHV and, thus, reduce the pool of infected cells available for subsequent reactivation and KS dissemination (analogous to immediate highly active antiretroviral therapy after occupational exposure to HIV). It is also possible that, by eliminating or limiting the number of KS cells that undergo KSHV lytic reactivation, ganciclovir could act to inhibit paracrine loops propagated by KSHV lytic proteins that contribute to local tumor development. And finally, the ganciclovir prodrug, after activation into its toxic metabolite by the virus (79), could result in direct cytotoxicity for the virally infected cells. To investigate the *in vivo* efficacy of ganciclovir against PEL, we tested its effect in the BCBL-1 xenograft model. Five mice were injected s.c. with 5×10^6 BCBL-1 and 0.2 ml Matrigel and left untreated with respect to drugs. A second cohort of 5 mice were injected i.p. first with 2 mg of Ganciclovir (Sigma-Aldrich) followed by 5×10^6 BCBL-1 with 0.2 ml of Matrigel s.c. (Table 1, Experiments #5 and #6). The 5 mice in the ganciclovir arm were given 2 mg of ganciclovir i.p. daily for 12 days. This follows our previously established dosing schedule that abrogates KSHV lytic replication in SCID-hu chimeric mice (64). Injection of ganciclovir at a site away from the tumor requires systemic dissemination of the drug for Ganciclovir to reach the tumor, rather than direct exposure of the tumor cells to the drug. All 5 of the

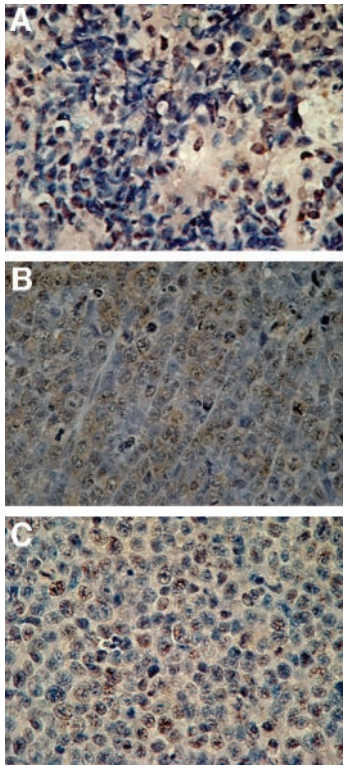

Fig. 3. LANA expression in BCBL-1 tumors. Thin sections were stained with a rat monoclonal antibody against the LANA protein (*brown*) and counterstained with hematoxylin (*blue*). *A*, a representative s.c. tumor. *B*, a representative i.p. tumor. *C*, a Matrigel-enhanced s.c. tumor. All images are at ×400 magnification.

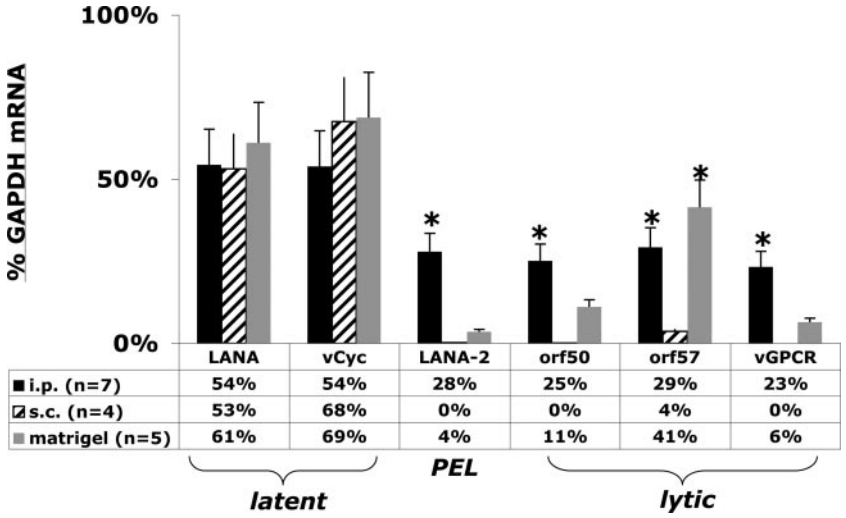

	LANA	vCyc	LANA-2	orf50	orf57	vGPCR
■ i.p. (n=7)	54%	54%	28%	25%	29%	23%
▨ s.c. (n=4)	53%	68%	0%	0%	4%	0%
■ matrigel (n=5)	61%	69%	4%	11%	41%	6%

latent *PEL* *lytic*

Fig. 4. Real-time quantitative PCR of KSHV gene expression in primary effusion lymphoma (*PEL*) tumors from xenografted SCID mice. Shown is a bar diagram of the levels (±SD) of KSHV mRNAs (LANA, vCYC, LANA-2, orf50, orf57, and vGPCR) in the three tumor classes: i.p., s.c., and s.c. plus Matrigel. The *number in brackets* is the total number of samples. The *vertical axis* indicates the relative level (in percent) of KSHV mRNAs to glyceraldehyde-3-phosphate dehydrogenase (*GAPDH*) mRNA in the tumor. * denotes a statistical difference of $P \leq 0.07$ between i.p. tumors and s.c. tumors. The table shows relative mRNA levels in percentage of GAPDH levels.

untreated control mice developed tumors. In a second experiment all of the mice developed tumors at the same time regardless of the presence or absence of ganciclovir (Table 1). Upon visual inspection, the tumors in the ganciclovir-treated cohort appeared smaller and seem to be associated with less angiogenesis (Fig. 5, *A–D*). This outcome suggests that ganciclovir may impede KSHV-dependent PEL lymphomagenesis but does not block tumor formation completely.

To validate our dosing regimen, we investigated the cytotoxic effects of ganciclovir on BCBL-1 cells in culture. Earlier studies had determined the concentration required to inhibit 50% of KSHV reactivation (IC_{50}) for ganciclovir to be 3.9 μM, and the concentration required to inhibit 90% of KSHV reactivation (IC_{90}) to be 39 μM (55, 71, 77). At these levels, ganciclovir does not exhibit any cellular cytotoxicity on uninfected cells in culture or cause toxicity in mice. On the basis of the known antiviral mechanism of action of ganciclovir, it is possible that the drug would kill cells in which KSHV reactivates, because during viral reactivation the viral kinases that are able to phosphorylate ganciclovir are expressed. To investigate this possibility, KSHV reactivation was induced in BCBL-1 cells in culture by transient (12 h) exposure to 20 ng/ml TPA before Ganciclovir exposure as described previously (52), and cell survival was recorded at 24, 48, and 96 h after induction (Fig. 6*A*). Upon TPA-induced KSHV reactivation, BCBL-1 cell growth ceased, and cells were destroyed by viral egress resulting in a net loss of cells over time (Fig. 6*A*, *second group*), whereas in contrast the untreated BCBL-1 cells grew exponentially as expected (Fig. 6*A*, *first group*). Treatment of BCBL-1 cells in culture with ganciclovir at 3.9 μM or 39 μM partially restored cell growth in BCBL-1 cells undergoing lytic reactivation as assessed by the counting of viable cells, presumably by interfering with viral maturation (Fig. 6*A*, *third* and *fourth group*). Only when BCBL-1 cells were treated with 390 μM (10 times the IC_{50}) was cytotoxicity observed (Fig. 6*A*, *fifth group*), which is consistent with the reported cytotoxicity concentration (CC_{50}) of ganciclovir on uninfected cells (77). These data demonstrate that even at the IC_{90} ganciclovir does not exhibit cellular cytotoxicity in PEL. Instead, the complete block of viral replication due to ganciclovir translates into increased survival of cells undergoing viral reactivation *in vitro*.

To investigate the mechanism of ganciclovir on viral transcription, we conducted viral array analysis using our previously validated real-time quantitative PCR array for KSHV (43, 72). Fig. 6*B* shows a heatmap representation of the normalized data, in which red indicated the highest and blue the lowest relative abundance for each KSHV mRNA under these experimental conditions. As expected (43), treatment with TPA alone induced most KSHV lytic transcripts, for instance the immediate early mRNAs (*e.g.*, orf57f1, orf57f2, orf50s1, and exon3, exon4, exon 3–4 of KbZIP). Treatment did not affect the latent mRNAs [orf72f1, 73–5′ untranslated region, Taq-F4 (for spliced vCyc), lat273, 71primer2], which fluctuate rather than showing a continues pattern. Addition of gancilovir at 4 and 40 μM increased the transcription of all of the lytic genes in a dose-dependent manner, presumably by inhibiting viral maturation and cellular destruction (as shown in Fig. 6*A*), which leads to an accumulation of immediate early, early, and delayed early mRNAs that were induced by TPA. Only at 400 μM ganciclovir, the CC_{50} for this drug, did we

Fig. 5. Gross anatomy of primary effusion lymphoma tumors in ganciclovir and mock-treated SCID mice. *A–D*, BCBL-1 plus Matrigel tumors in ganciclovir-treated mice. *E–H*, BCBL-1 plus Matrigel tumors in mock-treated mice.

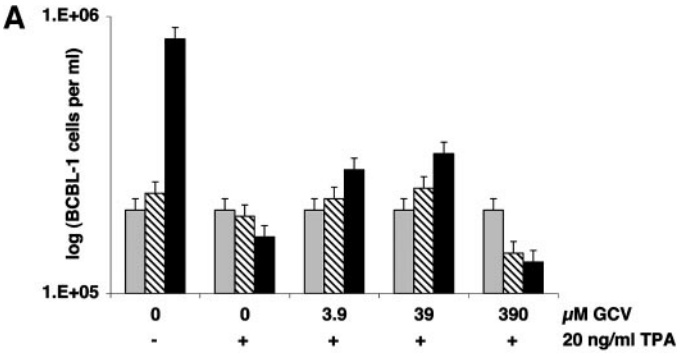

Fig. 6. *A*, effect of ganciclovir on BCBL-1 cell growth in culture. Depicted are the numbers of viable cells on a log scale at 12 (*gray*), 48 (*dashed*), or 96 (*black*) h after treatment with ganciclovir at the indicated concentration. Where indicated, BCBL-1 cells were incubated in the presence of 20 ng/ml TPA from 0 to 12 h. *B*, whole genome KSHV transcription profile in response to ganciclovir treatment. Shown is a heatmap representation of real-time quantitative reverse transcription-PCR results. Data, normalized to glyceraldehyde-3-phosphate dehydrogenase mRNA levels and median centered for each gene, which highlights relative changes in response to ganciclovir, rather than total mRNA levels. *Red* indicates increase, *blue* a decrease relative to the median (*black*).

observe a drastic decrease in virtually all of the viral mRNAs, as those virally infected cells that reactivate and phosphorylate the ganciclovir prodrug are removed from the culture. At this concentration the loss in cell viability (Fig. 6*A*) is mirrored by the loss of viral mRNAs.

DISCUSSION

Malignant lymphomas are common in late-stage AIDS patients and other immunosuppressed individuals, such as transplant recipients. In general, their prognosis is extremely poor. PELs represent an unusual and distinct set of AIDS-associated non-Hodgkin's lymphomas with a median patient survival of less than 6 months in most cohorts (80). They can present as solid masses, but most often as lymphomatous effusions in the body cavities. Hence, PELs were initially called BCBLs (34). Because PELs generally do not express B cell-lineage antigens (CD20; Ref. 36), they cannot be treated with B cell-specific immunotherapeutics. To date, only conventional anticancer chemotherapies are in use to treat patients with PEL. These tumors are distinct from other non-Hodgkin's lymphomas, however, due to their established association with the human γherpesvirus KSHV. All of the PEL cells contain >50 copies of the KSHV genome, and furthermore, all of the PEL cells express the KSHV latent genes LANA, v-cyclin, and v-FLIP (41–43, 48, 74), as well as LANA-2/vIRF-3, suggesting that KSHV is required for tumorigenesis. Additionally, in ~80% of PEL cases, the tumor cells are also infected with EBV. A principle bottleneck for mechanistic investigations into the role of KSHV in PEL tumorigenesis and for the evaluation of innovative drugs that specifically target the viral component of PEL is the lack of rapid and economically practical preclinical animal models. Most often, PEL cell lines are propagated in cell culture in the presence of a steady state of numerous media supplements, such as FCS, and so forth. This environment may stunt, alter, or redirect the virally infected cellular response to antitumor and antiviral drugs. In an effort to address these limitations and to capitalize upon KSHV as a unique tumor-specific target, we developed a rapid, quantitative xenograft model in SCID mice that allows us to monitor PEL growth continuously and noninvasively *in vivo*. This model provides a more natural tumor microenvironment compared with cell culture and should aid in the evaluation of novel therapeutics and tumor vaccines.

We found that Matrigel enables rapid s.c. growth of PEL, which lends itself to continuous, noninvasive monitoring of tumor progression. Matrigel provides a supporting extracellular lattice for individual

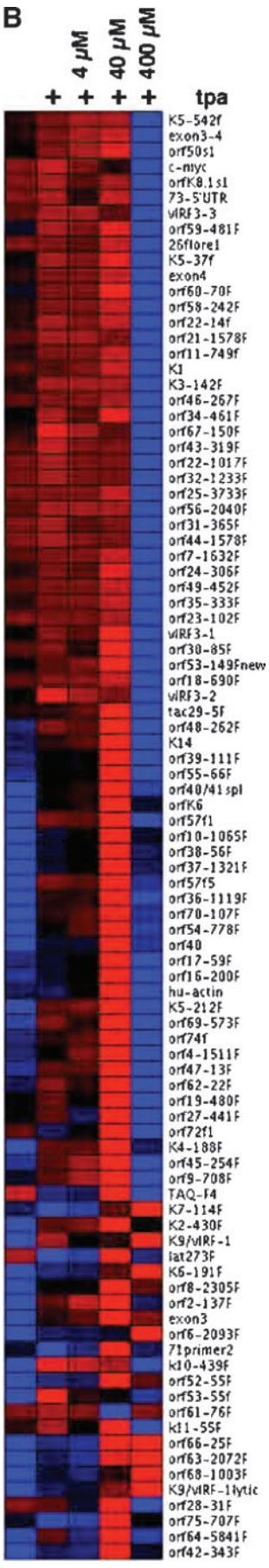

Fig. 6. *B, Continued.*

PEL cells. As a consequence, the tumors appear very homogenous, highly angiogenic, and maintain PEL morphology (Fig. 1). Whether the growth factor-depleted extracellular matrix additionally provides signals through direct contact with the cells as occurs during normal development is currently unresolved. KSHV was retained in the PEL tumor cells as evidenced by uniform LANA expression at both the mRNA and protein levels (Figs. 3 and 4). Without Matrigel, PEL did not grow in the s.c. environment within the time frame of our observation period. Rather, rare variants emerged after a very long *in vivo* incubation. They were characterized by disorganized growth, local necrosis, and altered viral gene transcription (Figs. 2–4) and, hence, would not be expected to mimic the human disease.

We found substantial evidence for KSHV lytic gene expression in PEL grown in the mouse xenograft model (Fig. 4). These data substantiate a paracrine modus operandi for KSHV pathogenesis that postulates that KSHV lytic genes, such as vGPCR/orf74 (31, 81, 82), in a portion of tumor cells contribute to tumor development as a whole. Presumably, LANA and the other KSHV latent oncogenes suffice to initiate B-cell transformation under optimal growth conditions in the presence of the progrowth environment (high endogenous interleukin 6 and chronic antigen stimulation) of the splenic mantle zone where KSHV-associated MCD can be found. The rich progrowth environment of the mantle zone is mimicked in current suspension cultures of PEL cell lines that include serum growth factors and endogenous, human interleukin 6. In contrast, KSHV lytic oncogenes would be needed to sustain ectopic pleural growth in advanced PEL. This dichotomy is mimicked in our mouse xenograft model by i.p. or s.c. plus Matrigel implantation. Studies to identify changes in cellular gene expression between these two microenvironments are currently ongoing.

We found increased transcription of KSHV lytic genes in the BCBL-1 xenografts (Fig. 4). This prompted us to investigate the susceptibility of such tumors to the antiviral drug ganciclovir, which requires activation by the viral thymidine kinase (TK/orf21) and/or the viral phosphotransferase (PT/orf36; Refs. 79, 83). Ganciclovir inhibits KSHV replication in BCBL-1 cells and SCID-hu mice (55, 64, 71, 76, 77). Investigations of the effect of ganciclovir on KSHV-associated PEL are warranted because the treatment of EBV-associated lymphomas with antiviral regimens has received renewed attention recently due to the predicted high therapeutic index and antitumor activity of these virus-specific drugs (69, 79, 84–88). Both EBV and KSHV encode a viral thymidine kinase (BXLF1 and orf21, respectively), which can phosphorylate ganciclovir, although the efficiency of this reaction compared with the thymidine kinase of the α and β herpesviruses is still under debate (79, 83, 86, 89–91). In the case of KSHV, the selectivity index for ganciclovir is 39 (77). Therefore, we hypothesized that the presence of these viral enzymes should results in the selective growth retardation of KSHV-infected cells (reviewed in Ref. 92). Furthermore, we hoped that, as in the case of combination nucleoside/gene-therapy in glioblastoma (93) where not every tumor cell needed to express the viral kinase, a significant bystander effect would be observed for PEL tumors. Contrary to our expectations, ganciclovir alone did not significantly inhibit tumor growth in the BCBL-1 xenograft model (Table 1) nor did it kill BCBL-1 cells after KSHV reactivation in culture (Fig. 6). Whole viral genome profiling showed that at the IC_{90} ganciclovir allowed for the sustained high level transcription of viral early genes by blocking completion of the viral life cycle. This suggests that the clinical effects of ganciclovir on KS as seen in a study of human CMV-induced retinitis (78) may be due to its systemic inhibition of KSHV lytic replication or reactivation, which can be caused by human cytomegalovirus (62), but not necessarily a direct antitumor effect. Alternatively, KS lesions may exhibit a still greater proportion of cells expressing lytic genes or are capable to support more complete viral replication than typically seen in PEL cell lines, which renders them susceptible to treatment with this drug. We previously documented extreme heterogeneity of viral transcription in primary KS biopsies (72), which provide a rationale for tumor stratification in additional studies.

ACKNOWLEDGMENTS

We thank William Harrington and Blossom Damania for discussion and critical reading of the manuscript.

REFERENCES

1. Antman K, Chang Y. Kaposi's sarcoma. N Engl J Med 2000;342:1027–38.
2. Ablashi DV, Chatlynne LG, Whitman, JE Jr, Cesarman, E. Spectrum of Kaposi's sarcoma-associated herpesvirus, or human herpesvirus 8, diseases Clin Microbiol Rev 2002;15:439–64.
3. Cesarman E, Moore PS, Rao PH, Inghirami G, Knowles DM, Chang Y. In vitro establishment and characterization of two acquired immunodeficiency syndrome-related lymphoma cell lines (BC-1 and BC-2) containing Kaposi's sarcoma-associated herpesvirus-like (KSHV) DNA sequences. Blood 1995;86:2708–14.
4. Soulier J, Grollet L, Oksenhendler E, et al. Kaposi's sarcoma-associated herpesvirus-like DNA sequences in multicentric Castleman's disease [see comments]. Blood 1995;86:1276–80.
5. Russo JJ, Bohenzky RA, Chien MC, et al. Nucleotide sequence of the Kaposi sarcoma-associated herpesvirus (HHV8). Proc Natl Acad Sci USA 1996;93:14862–7.
6. Neipel F, Albrecht JC, Fleckenstein B. Cell-homologous genes in the Kaposi's sarcoma-associated rhadinovirus human herpesvirus 8: determinants of its pathogenicity? J Virol 1997;71:4187–92.
7. Nicholas J, Zong JC, Alcendor DJ, et al. Novel organizational features, captured cellular genes, and strain variability within the genome of KSHV/HHV8. J. Natl. Cancer Inst Monogr 1998;79–88.
8. Boshoff C, Schulz TF, Kennedy MM, et al. Kaposi's sarcoma-associated herpesvirus infects endothelial and spindle cells Nat Med 1995;1:1274–8.
9. Li JJ, Huang YQ, Cockerell CJ, Friedman-Kien AE. Localization of human herpes-like virus type 8 in vascular endothelial cells and perivascular spindle-shaped cells of Kaposi's sarcoma lesions by in situ hybridization. Am J Pathol 1996;148:1741–8.
10. Staskus KA, Zhong W, Gebhard K, et al. Kaposi's sarcoma-associated herpesvirus gene expression in endothelial (spindle) tumor cells. J Virol 1997;71:715–9.
11. Sturzl M, Blasig C, Schreier A, et al. Expression of HHV-8 latency-associated T0.7 RNA in spindle cells and endothelial cells of AIDS-associated, classical and African Kaposi's sarcoma. Int J Cancer 1997;72:68–71.
12. Dittmer D, Lagunoff M, Renne R, Staskus K, Haase A, Ganem D. A cluster of latently expressed genes in Kaposi's sarcoma-associated herpesvirus. J Virol 1998;72:8309–15.
13. Rabkin CS, Janz S, Lash A, et al. Monoclonal origin of multicentric Kaposi's sarcoma lesions [see comments]. N Engl J Med 1997;336:988–93.
14. Judde JG, Lacoste V, Briere J, et al. Monoclonality or oligoclonality of human herpesvirus 8 terminal repeat sequences in Kaposi's sarcoma and other diseases [see comments]. J Natl Cancer Inst 2000;92:729–36.
15. Gill PS, Tsai YC, Rao AP, et al. Evidence for multiclonality in multicentric Kaposi's sarcoma. Proc Natl Acad Sci USA 1998;95:8257–61.
16. Flamand L, Zeman RA, Bryant JL, Lunardi-Iskandar Y, Gallo RC. Absence of human herpesvirus 8 DNA sequences in neoplastic Kaposi's sarcoma cell lines. J Acquir Immune Defic Syndr Hum Retrovirol 1996;13:194–7.
17. Lebbe C, de Cremoux P, Millot G, et al. Characterization of in vitro culture of HIV-negative Kaposi's sarcoma-derived cells. In vitro responses to alfa interferon. Arch Dermatol Res 1997;289:421–8.
18. Pati S, Foulke JS Jr, Barabitskaya O, et al. Human herpesvirus 8-encoded vGPCR activates nuclear factor of activated T cells and collaborates with human immunodeficiency virus type 1 Tat. J Virol 2003;77:5759–73.
19. Samaniego F, Markham PD, Gallo RC, Ensoli B. Inflammatory cytokines induce AIDS-Kaposi's sarcoma-derived spindle cells to produce and release basic fibroblast growth factor and enhance Kaposi's sarcoma-like lesion formation in nude mice. J Immunol 1995;154:3582–92.
20. Renne R, Blackbourn D, Whitby D, Levy J, Ganem D. Limited transmission of Kaposi's sarcoma-associated herpesvirus in cultured cells. J Virol 1998;72:5182–8.
21. Gallo RC. The enigmas of Kaposi's sarcoma. Science 1998;282:1837–9.
22. Moses AV, Fish KN, Ruhl R, Smith PP, Strussenberg JG, Zhu L, Chandran B, Nelson JA. Long-term infection and transformation of dermal microvascular endothelial cells by human herpesvirus 8. J Virol 1999;73:6892–902.
23. Ciufo DM, Cannon JS, Poole LJ, et al. Spindle cell conversion by Kaposi's sarcoma-associated herpesvirus: formation of colonies and plaques with mixed lytic and latent gene expression in infected primary dermal microvascular endothelial cell cultures. J Virol 2001;75:5614–26.
24. Lagunoff M, Bechtel J, Venetsanakos E, et al. De novo infection and serial transmission of Kaposi's sarcoma-associated herpesvirus in cultured endothelial cells. J Virol 2002;76:2440–8.
25. Bechtel JT, Liang Y, Hvidding J, Ganem D. Host range of Kaposi's sarcoma-associated herpesvirus in cultured cells. J Virol 2003;77:6474–81.
26. Flore O, Rafii S, Ely S, O'Leary JJ, Hyjek EM, Cesarman E. Transformation of primary human endothelial cells by Kaposi's sarcoma- associated herpesvirus. Nature 1998;394:588–92.

27. Ganem D. KSHV and Kaposi's sarcoma: the end of the beginning? Cell 1997;91: 157–60.
28. Hayward GS. Initiation of angiogenic Kaposi's sarcoma lesions. Cancer Cell 2003; 3:1–3.
29. Boshoff C, Weiss RA. Aetiology of Kaposi's sarcoma: current understanding and implications for therapy. Mol Med Today 1997;3:488–94.
30. Herndier B, Ganem D. The biology of Kaposi's sarcoma. Cancer Treat Res 2001; 104:89–126.
31. Cesarman E, Mesri EA, Gershengorn MC. Viral G protein-coupled receptor and Kaposi's sarcoma: a model of paracrine neoplasia? [comment]. J Exp Med 2000;191: 417–22.
32. Gaidano G, Cechova K, Chang Y, Moore PS, Knowles DM, Dalla-Favera R. Establishment of AIDS-related lymphoma cell lines from lymphomatous effusions. Leukemia 1996;10:1237–40.
33. Komanduri KV, Luce JA, McGrath MS, Herndier BG, Ng VL. The natural history and molecular heterogeneity of HIV-associated primary malignant lymphomatous effusions. J Acquir Immune Defic Syndr Hum Retrovirol 1996;13:215–26.
34. Herndier BG, Werner A, Arnstein P, et al. Characterization of a human Kaposi's sarcoma cell line that induces angiogenic tumors in animals. Aids 1994;8:575–81.
35. Picchio GR, Sabbe RE, Gulizia RJ, McGrath M, Herndier BG, Mosier DE. The KSHV/HHV8-infected BCBL-1 lymphoma line causes tumors in SCID mice but fails to transmit virus to a human peripheral blood mononuclear cell graft. Virology 1997;238:22–9.
36. Arvanitakis L, Mesri EA, Nador RG, et al. Establishment and characterization of a primary effusion (body cavity- based) lymphoma cell line (BC-3) harboring kaposi's sarcoma-associated herpesvirus (KSHV/HHV-8) in the absence of Epstein-Barr virus. Blood 1996;88:2648–54.
37. Cannon JS, Ciufo D, Hawkins AL, et al. A new primary effusion lymphoma-derived cell line yields a highly infectious Kaposi's sarcoma herpesvirus-containing supernatant [In Process Citation]. J Virol 2000;74:10187–93.
38. Katano H, Hoshino Y, Morishita Y, et al. Establishing and characterizing a CD30-positive cell line harboring HHV-8 from a primary effusion lymphoma. J Med Virol 1999;58:394–401.
39. Boshoff C, Gao SJ, Healy LE, et al. Establishing a KSHV+ cell line (BCP-1) from peripheral blood and characterizing its growth in Nod/SCID mice. Blood 1998;91: 1671–9.
40. Cesarman E, Nador RG, Aozasa K, Delsol G, Said JW, Knowles DM. Kaposi's sarcoma-associated herpesvirus in non-AIDS related lymphomas occurring in body cavities. Am J Pathol 1996;149:53–7.
41. Paulose-Murphy M, Ha NK, Xiang C, et al. Transcription program of human herpesvirus 8 (kaposi's sarcoma-associated herpesvirus). J Virol 2001;75:4843–53.
42. Jenner RG, Alba MM, Boshoff C, Kellam P. Kaposi's sarcoma-associated herpesvirus latent and lytic gene expression as revealed by DNA arrays. J Virol 2001;75:891–902.
43. Fakhari FD, Dittmer DP. Charting latency transcripts in kaposi's sarcoma-associated herpesvirus by whole-genome real-time quantitative PCR. J Virol 2002; 76:6213–23.
44. Rainbow L, Platt GM, Simpson GR, et al. The 222- to 234-kilodalton latent nuclear protein (LNA) of Kaposi's sarcoma-associated herpesvirus (human herpesvirus 8) is encoded by orf73 and is a component of the latency-associated nuclear antigen. J Virol 1997;71:5915–21.
45. Kedes DH, Lagunoff M, Renne R, Ganem D. Identification of the gene encoding the major latency-associated nuclear antigen of the Kaposi's sarcoma-associated herpesvirus. J Clin Investig 1997;100:2606–10.
46. Kellam P, Boshoff C, Whitby D, Matthews S, Weiss RA, Talbot SJ. Identification of a major latent nuclear antigen, LNA-1, in the human herpesvirus 8 genome. J Hum Virol 1997;1:19–29.
47. Kellam P, Bourboulia D, Dupin N, et al. Characterization of monoclonal antibodies raised against the latent nuclear antigen of human herpesvirus 8. J Virol 1999;73: 5149–55.
48. Dupin N, Fisher C, Kellam P, et al. Distribution of human herpesvirus-8 latently infected cells in Kaposi's sarcoma, multicentric Castleman's disease, and primary effusion lymphoma. Proc Natl Acad Sci USA 1999;96:4546–51.
49. Rivas C, Thlick AE, Parravicini C, Moore PS, Chang Y. Kaposi's sarcoma-associated herpesvirus LANA2 is a B-cell-specific latent viral protein that inhibits p53. J Virol 2001;75:429–38.
50. Renne R, Lagunoff M, Zhong W, Ganem D. The size and conformation of Kaposi's sarcoma-associated herpesvirus (human herpesvirus 8) DNA in infected cells and virions. J Virol 1996;70:8151–4.
51. Carbone A, Gloghini A, Vaccher E, et al. Kaposi's sarcoma-associated herpesvirus DNA sequences in AIDS-related and AIDS-unrelated lymphomatous effusions. Br J Haematol 1996;94:533–43.
52. Renne R, Zhong W, Herndier B, et al. Lytic growth of Kaposi's sarcoma-associated herpesvirus (human herpesvirus 8) in culture. Nat Med 1996;2:342–6.
53. Matsushima AY, Strauchen JA, Lee G, et al. Posttransplantation plasmacytic proliferations related to Kaposi's sarcoma-associated herpesvirus. Am J Surg Pathol 1999;23:1393–400.
54. Strauchen JA, Hauser AD, Burstein D, Jimenez R, Moore PS, Chang Y. Body cavity-based malignant lymphoma containing Kaposi sarcoma-associated herpesvirus in an HIV-negative man with previous Kaposi sarcoma. Ann Intern Med 1996;125: 822–5.
55. Zoeteweij JP, Eyes ST, Orenstein JM, et al. Identification and rapid quantification of early- and late-lytic human herpesvirus 8 infection in single cells by flow cytometric analysis: characterization of antiherpesvirus agents. J Virol 1999;73: 5894–902.
56. Miller G, Heston L, Grogan E, et al. Selective switch between latency and lytic replication of Kaposi's sarcoma herpesvirus and Epstein-Barr virus in dually infected body cavity lymphoma cells. J Virol 1997;71:314–24.
57. Sun R, Lin SF, Staskus K, et al. Kinetics of Kaposi's sarcoma-associated herpesvirus gene expression. J Virol 1999;73:2232–42.
58. Yu Y, Black JB, Goldsmith CS, Browning PJ, Bhalla K, Offermann MK. Induction of human herpesvirus-8 DNA replication and transcription by butyrate and TPA in BCBL-1 cells. J Gen Virol 1999;80:83–90.
59. Salahuddin SZ, Nakamura S, Biberfeld P, et al. Angiogenic properties of Kaposi's sarcoma-derived cells after long-term culture in vitro. Science 1988;242:430–3.
60. Chang J, Renne R, Dittmer D, Ganem D. Inflammatory cytokines and the reactivation of Kaposi's Sarcoma- associated herpesvirus lytic replication. Virology 2000;266: 17–25.
61. Mercader M, Taddeo B, Panella JR, Chandran B, Nickoloff BJ, Foreman KE. Induction of HHV-8 lytic cycle replication by inflammatory cytokines produced by HIV-1-infected T cells. Am J Pathol 2000;156:1961–71.
62. Vieira J, O'Hearn P, Kimball L, Chandran B, Corey L. Activation of Kaposi's sarcoma-associated herpesvirus (human herpesvirus 8) lytic replication by human cytomegalovirus. J Virol 2001;75:1378–86.
63. Mesri EA, Cesarman E, Arvanitakis L, et al. Human herpesvirus-8/Kaposi's sarcoma-associated herpesvirus is a new transmissible virus that infects B cells. J Exp Med 1996;183:2385–90.
64. Dittmer D, Stoddart C, Renne R, et al. Experimental Transmission of Kaposi's Sarcoma-associated Herpesvirus (KSHV/HHV-8) to SCID-hu Thy/Liv Mice. J Exp Med 1999;190:1857–68.
65. Foreman KE, Friborg J, Chandran B, et al. Injection of human herpesvirus-8 in human skin engrafted on SCID mice induces Kaposi's sarcoma-like lesions. J Dermatol Sci 2001;26:182–93.
66. Zenger E, Abbey NW, Weinstein MD, et al. Injection of human primary effusion lymphoma cells or associated macrophages into severe combined immunodeficient mice causes murine lymphomas. Cancer Res 2002;62:5536–42.
67. Said JW, Chien K, Tasaka T, Koeffler HP. Ultrastructural characterization of human herpesvirus 8 (Kaposi's sarcoma-associated herpesvirus) in Kaposi's sarcoma lesions: electron microscopy permits distinction from cytomegalovirus (CMV). J Pathol 1997;182:273–81.
68. Kliche S, Kremmer E, Hammerschmidt W, Koszinowski U, Haas J. Persistent infection of Epstein-Barr virus-positive B lymphocytes by human herpesvirus 8. J Virol 1998;72:8143–9.
69. Westphal EM, Blackstock W, Feng W, Israel B, Kenney SC. Activation of lytic Epstein-Barr virus (EBV) infection by radiation and sodium butyrate in vitro and in vivo: a potential method for treating EBV-positive malignancies. Cancer Res 2000; 60:5781–8.
70. Teicher B. (ed.) Tumor Models in Cancer Research. Totowa: Humana Press, 2002.
71. Kedes DH, Ganem D. Sensitivity of Kaposi's sarcoma-associated herpesvirus replication to antiviral drugs. Implications for potential therapy. J Clin Investig 1997;99: 2082–6.
72. Dittmer DP. Transcription profile of Kaposi's sarcoma-associated herpesvirus in primary Kaposi's sarcoma lesions as determined by real-time PCR arrays. Cancer Res 2003;63:2010–5.
73. Manniatis I. Molecular Cloning. Cold Spring Harbor; Cold Spring Harbor Laboratory Press, 1999.
74. Sarid R, Flore O, Bohenzky RA, Chang Y, Moore PS. Transcription mapping of the Kaposi's sarcoma-associated herpesvirus (human herpesvirus 8) genome in a body cavity-based lymphoma cell line (BC-1). J Virol 1998;72:1005–12.
75. Jeong J, Papin J, Dittmer D. Differential Regulation of the overlapping Kaposi's Sarcoma-associated Herpesvirus (KSHV/HHV-8) vGCR (orf74) and LANA (orf73) promoter. J Virology 2001;75:1798–807.
76. Medveczky MM, Horvath E, Lund T, Medveczky PG. In vitro antiviral drug sensitivity of the Kaposi's sarcoma-associated herpesvirus. Aids 1997;11:1327–32.
77. Neyts J, De Clercq E. Antiviral drug susceptibility of human herpesvirus 8. Antimicrob Agents Chemother 1997;41:2754–6.
78. Martin DF, Kuppermann BD, Wolitz RA, Palestine AG, Li H, Robinson CA. Oral ganciclovir for patients with cytomegalovirus retinitis treated with a ganciclovir implant. Roche Ganciclovir Study Group [see comments]. N Engl J Med 1999;340: 1063–70.
79. Cannon JS, Hamzeh F, Moore S, Nicholas J, Ambinder RF. Human herpesvirus 8-encoded thymidine kinase and phosphotransferase homologues confer sensitivity to ganciclovir. J Virol 1999;73:4786–93.
80. Boulanger E, Agbalika F, Maarek O, et al. A clinical, molecular and cytogenetic study of 12 cases of human herpesvirus 8 associated primary effusion lymphoma in HIV-infected patients. Hematol J 2001;2:172–9.
81. Bais C, Santomasso B, Coso O, et al. G-protein-coupled receptor of Kaposi's sarcoma-associated herpesvirus is a viral oncogene and angiogenesis activator [see comments] [published erratum appears in Nature 1998 Mar 12;392(6672):210]. Nature 1998;391:86–9.
82. Montaner S, Sodhi A, Molinolo A, et al. Endothelial infection with KSHV genes in vivo reveals that vGPCR initiates Kaposi's sarcomagenesis and can promote the tumorigenic potential of viral latent genes. Cancer Cell 2003;3:23–36.
83. Gustafson EA, Schinazi RF, Fingeroth JD. Human herpesvirus 8 open reading frame 21 is a thymidine and thymidylate kinase of narrow substrate specificity that efficiently phosphorylates zidovudine but not ganciclovir. J Virol 2000;74: 684–92.
84. Roychowdhury S, Peng R, Baiocchi RA, et al. Experimental treatment of Epstein-Barr virus-associated primary central nervous system lymphoma. Cancer Res 2003; 63:965–71.

85. Lee RK, Cai JP, Deyev V, et al. Azidothymidine and interferon-alpha induce apoptosis in herpesvirus- associated lymphomas. Cancer Res 1999;59: 5514–20.
86. Moore SM, Cannon JS, Tanhehco YC, Hamzeh FM, Ambinder RF. Induction of Epstein-Barr virus kinases to sensitize tumor cells to nucleoside analogues. Antimicrob Agents Chemother 2001;45:2082–91.
87. Faller DV, Mentzer SJ, Perrine SP. Induction of the Epstein-Barr virus thymidine kinase gene with concomitant nucleoside antivirals as a therapeutic strategy for Epstein-Barr virus-associated malignancies. Curr Opin Oncol 2001;13:360–7.
88. Feng WH, Israel B, Raab-Traub N, Busson P, Kenney SC. Chemotherapy induces lytic EBV replication and confers ganciclovir susceptibility to EBV-positive epithelial cell tumors. Cancer Res 2002;62:1920–6.
89. Gustafson EA, Chillemi AC, Sage DR, Fingeroth JD. The Epstein-Barr virus thymidine kinase does not phosphorylate ganciclovir or acyclovir and demonstrates a narrow substrate specificity compared to the herpes simplex virus type 1 thymidine kinase. Antimicrob Agents Chemother 1998;42:2923–31.
90. Littler E, Zeuthen J, McBride AA, et al. Identification of an Epstein-Barr virus-coded thymidine kinase. EMBO J 1986;5:1959–66.
91. Littler E, Arrand JR. Characterization of the Epstein-Barr virus-encoded thymidine kinase expressed in heterologous eucaryotic and procaryotic systems. J Virol 1988; 62:3892–5.
92. Staudt MR, Dittmer DP. Viral latent proteins as targets for Kaposi's sarcoma and Kaposi's sarcoma-associated herpesvirus (KSHV/HHV-8) induced lymphoma. Curr Drug Targets Infect Disord 2003;3:129–35.
93. Rubsam LZ, Boucher PD, Murphy PJ, KuKuruga M, Shewach DS. Cytotoxicity and accumulation of ganciclovir triphosphate in bystander cells cocultured with herpes simplex virus type 1 thymidine kinase-expressing human glioblastoma cells. Cancer Res 1999;59:669–75.